ELSEVIER

Polymer 40 (1998) 183–192

polymer

The length of cooperativity at the glass transition in poly(vinyl acetate) from the modeling of the structural relaxation process

J.L. Gómez Ribelles[a,*], A. Vidaurre Garayo[b], J.M.G. Cowie[c], R. Ferguson[c], S. Harris[c], I.J. McEwen[c]

[a]*Depto. de Termodinámica Aplicada, Universidad Politécnica de Valencia, P.O. Box 22012, E-46071 Valencia, Spain*
[b]*Depto. de Física Aplicada, Universidad Politécnica de Valencia, P.O. Box 22012, E-46071 Valencia, Spain*
[c]*Department of Chemistry, Heriot-Watt University, Riccarton, Edinburgh EH14 4AS, UK*

Received 24 October 1997; accepted 5 March 1998

Abstract

The structural relaxation process of poly(vinyl acetate) has been studied by differential scanning calorimetry. The sample was subjected to different thermal treatments including an isothermal annealing at temperature T_a for a time t_a. The heat capacity $c_p(T)$ was measured during a heating scan. Thus, the experimental results consist of a series of $c_p(T)$ curves determined after thermal histories with different values of T_a and t_a. The experimental results were compared with the prediction of a multiparameter phenomenological model described in references [15,16]. This model follows the evolution of the configurational entropy of the sample during the whole thermal history. The parameters of the model were calculated by simultaneous fits to five $c_p(T)$ curves, corresponding to different thermal histories (the parameters of the model have the character of material parameters, independent of the thermal history). This allows the determination of the temperature dependence of the relaxation times and the β parameter of the Kohlrausch–Williams–Watts equation. From these parameters and an estimate of the internal rotational barrier obtained by molecular mechanics calculations, the size of the smallest cooperative rearranging region in the Adam–Gibbs theory was calculated. This result is compared with the length of cooperativity calculated from the temperature fluctuation theory proposed by Donth.

Keywords: Glass transition; Structural relaxation; Physical ageing

1. Introduction

The relaxation processes in undercooled liquids at temperatures around and above the glass transition are determined by the cooperative rearrangements of its molecules or polymer chain segments. The extent of such intermolecular correlations can be characterized by a length scale that has been estimated from different experimental or theoretical approaches [1–3]. The values given in the literature for this characteristic length at the glass transition temperature, T_g, range between molecular dimensions and 1 or 2 nm.

The Adam and Gibbs theory [4] is another possible approach to the estimation of the length of cooperativity. The theory is based on the definition of a cooperative rearranging region, CRR, in which a conformational transition may take place with no interaction with the rest of the material. The average probability of a conformational rearrangement is calculated in terms of the number of molecules or polymer segments contained in the smallest CRR allowing a conformational rearrangement, z^*, and the free energy barrier per molecule or chain segment hindering the cooperative rearrangement, $\Delta\mu$:

$$\bar{W}(T) = A\exp\frac{z^*\Delta\mu}{kT}, \tag{1}$$

where k is Boltzmann's constant. The parameter z^* can be used to characterise the length of cooperativity.

The microscopic parameters in Eq. (1) can be related to the macroscopic configurational entropy $S_c(T)$, from Adam and Gibbs [4]:

$$\frac{S_c(T)M_s}{N_A} = \frac{s_c^*}{z^*(T)} \tag{2}$$

here $s_c^* = k\ln\Omega^*$ is the configurational entropy of the smallest CRR (with Ω^* being the number of states available for this smallest CRR). $S_c(T)$ is expressed in specific entropy units ($J\,g^{-1}\,K^{-1}$), M_s is the molecular weight of the unit responsible for the cooperative rearrangement and N_A is Avogadro's number.

* Corresponding author.

0032-3861/98/$ - see front matter
PII: S0032-3861(98)00213-4

In this framework, Adam and Gibbs [4] deduced the expression for the viscoelastic or dielectric relaxation times at temperatures above T_g:

$$\tau_{AG}(T) = A\exp\left(\frac{B}{TS_c(T)}\right), \tag{3}$$

where

$$B = \frac{\Delta\mu N_A s_c^*}{kM_s} = \frac{\Delta\mu' s_c^*}{kM_s}, \tag{4}$$

$\Delta\mu'$ being the free energy barrier per mol of molecules or main-chain polymer segments. From an experimental determination of $\tau_{AG}(T)$ and $S_c(T)$ it is possible to estimate the product $\Delta\mu z^*(T)$ using Eqs. (2) and (4). The calculation of z^* needs, in addition, a theoretical calculation of $\Delta\mu$. From this kind of approach and using the Vogel–Fulcher–Tammann–Hesse (VFTH) equation, which can be expressed as:

$$\tau = \tau_0\exp\frac{C}{T-T_0} = \tau_0\exp\frac{DT_0}{T-T_0} \tag{5}$$

Miller [5] deduced that, at T_g, $z^*(T_g) = T_g/(T_g - T_0)$. The proportionality between $z^*(T_g)$ and $T_g/(T_g - T_0)$ has been also proposed by Hodge [7].

The temperature dependence of the relaxation times of the conformational rearrangements can also be obtained from differential scanning calorimetry (DSC) through the modelling of the structural relaxation process. Structural relaxation is the term that designates the process of approach to an equilibrium state undergone by a glass held at constant environmental conditions after its formation history [6,7]. The glass transition itself is the result of the exponential dependence of the structural relaxation times on temperature. This is why the modelling of the structural relaxation is important and has attracted the attention of many research groups in the past decades (see for instance the recent reviews of references [7–10]). Phenomenological models contain a series of parameters that in most cases play the role of material constants in the deductions leading to the model equations. The set of model parameters can be determined by least-squares fitting to the experimental results. In differential scanning calorimetry (DSC) experiments, these results consist of a series of heat capacity, $c_p(T)$, curves measured in heating scans from a temperature T_{lower} below the glass transition temperature T_g to a temperature T_{upper} above T_g. Previously, the sample has been subjected to a thermal treatment that starts at T_{upper} with the sample in equilibrium, and may include, or not, an isothermal stage at an annealing temperature T_a for an annealing time t_a. The essential test for the validity of a phenomenological model is to check whether or not the set of model parameters are, in fact, material parameters, i.e. whether or not the model with a single set of parameters is able to reproduce the $c_p(T)$ curves measured after different thermal histories. Several studies have shown that this is not easy in the case of the Scherer–Hodge (SH) [11,12] or Narayanaswamy–Moynihan (NM) [13,14] models. Several possible causes of this problem have been suggested, with reference to the failure of some of the assumptions of these models.

Recently, a model has been proposed that introduces a new hypothesis related to the state attained at infinite time in the structural relaxation process at a temperature T_a [15,16]. This limit state is identified in the SH or NM models with the extrapolation to T_a of the equilibrium line experimentally determined above T_g. This is simply a result of the identification of the limit value of the fictive temperature T_f at infinite time with T_a. To introduce a different hypothesis with regard to this point, the equations of the model in references [15,16] are expressed in terms of the configurational entropy of the system $S_c(t)$ instead of the fictive temperature $T_f(t)$. The model keeps the main assumptions of the SH model but is able to introduce different expressions for the function $S_c^{lim}(T_a)$, the value of the configurational entropy attained at infinite time in an isothermal treatment at temperature T_a in the glassy state. We will call $S_c^{eq}(T)$ the extrapolation of the configurational entropy equilibrium line determined at temperatures above T_g to T (see Fig. 1a). The details of the model and the arguments given to justify its hypothesis have been discussed elsewhere [15–19] and will not be repeated here. Only the main equations will be included. For the numerical simulation, the cooling and heating stages of the thermal history are replaced by a series of one-degree steps, followed by isothermal stages with a duration calculated to give the same average rate of temperature change as in the experiments. The value of the configurational entropy at a time instant, t, after a series of temperature steps is:

$$S_c(t) = S_c^{lim}(T) - \sum_{i=1}^{n}\left(\int_{T_{i-1}}^{T_i}\frac{\Delta c_p^{lim}(T)}{T}dT\right)\cdot\phi(u(t)-u(t_{i-1})). \tag{6}$$

where $u(t)$ is a reduced time:

$$u(t) = \int_0^t \frac{d\sigma}{\tau(\sigma)}, \tag{7}$$

and ϕ is a relaxation function of the Kohlraush–Williams–Watts type:

$$\phi(u) = \exp(-u^\beta). \tag{8}$$

In Eq. (6), $\Delta c_p^{lim}(T) = c_p^{lim}(T) - c_{pg}(T)$ ($c_{pg}(T)$ being the heat capacity in the glassy state) is the configurational heat capacity in the relaxed state, which is defined through:

$$S_c^{lim}(T_i) - S_c^{lim}(T_{i-1}) = \int_{T_{i-1}}^{T_i}\frac{\Delta c_p^{lim}(T)}{T}dT. \tag{9}$$

Thus, if T^* is a temperature above the glass transition region, then for any temperature T in the glass transition temperature interval or below:

$$S_c^{lim}(T) = S_c^{eq}(T^*) + \int_{T^*}^{T}\frac{\Delta c_p^{lim}(\theta)}{\theta}d\theta. \tag{10}$$

The shape of $S_c^{lim}(T)$ and $c_p^{lim}(T)$ are shown in Fig. 1. The

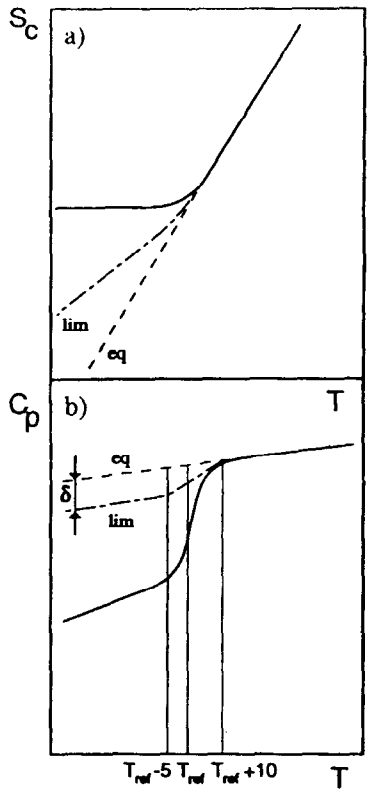

Fig. 1. (a) Sketch of the configurational entropy corresponding to the liquid state (dashed line), to an experimental cooling scan at a finite cooling rate (solid line), and to the hypothetical line of the limit states of the structural relaxation process (dashed-dotted line). (b) $c_p(T)$ lines corresponding to the three cases described in (a): the dashed line corresponds to the liquid state $c_{pl}(T)$, the solid line corresponds to an experimental cooling scan, and the dashed-dotted line corresponds to the specific heat capacity in the limit states of the structural relaxation process: $c_p^{lim}(T)$

slope of $S_c^{lim}(T)$ is smaller than that of $S_c^{eq}(T)$ at temperatures below the glass transition interval. The change of slope is gradual, covering a temperature interval of 15°C around a certain reference temperature that, in this work, will be identified with the glass transition temperature, determined as the intersection point of the liquid and glassy enthalpy lines, as determined from the scan measured after cooling the sample at 40°C min^{-1} from a temperature above the glass transition. In this way, the shape of $S_c^{lim}(T)$ is defined with a single additional parameter, called δ, that measures in some way the difference of slope of $S_c^{eq}(T)$ and $S_c^{lim}(T)$.

We assume for τ, a dependence on the instantaneous values of configurational entropy and temperature given by the Adam and Gibbs equation [4]:

$$\tau(S_c, T) = A\exp\left(\frac{B}{S_c T}\right). \tag{11}$$

Eq. (11) is an extension of Adam and Gibbs' expression [4] for the equilibrium relaxation times to states out of equilibrium. When the configurational entropy S_c has the equilibrium value $S_c^{eq}(T)$ we have:

$$\tau^{eq}(T) = A\exp\left(\frac{B}{S_c^{eq}(T)T}\right) \tag{12}$$

and for the configurational entropy in equilibrium states:

$$S_c^{eq}(T) = \int_{T_2}^{T} \frac{\Delta c_p(\theta)}{\theta} d\theta \tag{13}$$

is valid. In this equation, T_2 is the Gibbs–DiMarzio transition temperature [20], $\Delta c_p(T) = c_{pl}(T) - c_{pg}(T)$ is the configurational heat capacity, and c_{pl} is the heat capacity in the liquid state.

The model proposed in references [15,16] has been successfully applied to several polymers, including polycarbonate [15], poly(ether imide) [16], polystyrene and some polystyrene derivatives [17], an epoxy resin [18] and a styrene–acrylonitrile copolymer [19]. In all these polymers it has been found that the introduction of the new hypothesis on the limit states of the structural relaxation model improves significantly the fit of the experimental results. The model with a single set of model parameters is able to reproduce a broad series of $c_p(T)$ curves measured after thermal histories quite different to each other. On the contrary, if, in the model equations, the value of δ is kept equal to 0 (this implies that $S_c^{lim}(T) = S_c^{eq}(T)$ and the model prediction is very similar to that of the SH model), the least squares search routine is not able to find a set of parameters which reproduce simultaneously all the experimental curves.

The aim of this work is to explore the relationship between the fitting parameters of the phenomenological model and the microscopic parameters of the Adam–Gibbs theory, in particular the number of main chain segments contained in the smallest cooperative rearranging region (CRR) and the number of states available to it.

2. Experimental

The poly(vinyl acetate) used was a secondary standard from Aldrich; M_n = 52 700 g mol^{-1}, polydispersity index 2.4. Prior to use, the sample was dried rigorously in a vacuum oven above its T_g. No further purification was carried out. ^{1}H n.m.r. analysis showed that the sample contained 26% syndio-, 26% iso- and 48% hetero-tactic dyads.

The differential scanning calorimetry, DSC, experiments were carried out in a Perkin–Elmer DSC-2 differential scanning calorimeter. All the experiments started at T_g + 50 K with the sample in equilibrium. The sample was then cooled down to the ageing temperature T_a at a rate of 40 K min^{-1}, kept at this temperature for a time t_a, and cooled down again at 40 K min^{-1} until reaching T_g − 60 K. Then the measuring scan was carried out at 20 K min^{-1} until T_g + 40 K (approximately seven data points are loaded each degree during the measuring scan but only one datum point per degree is shown on the figures). The results are presented

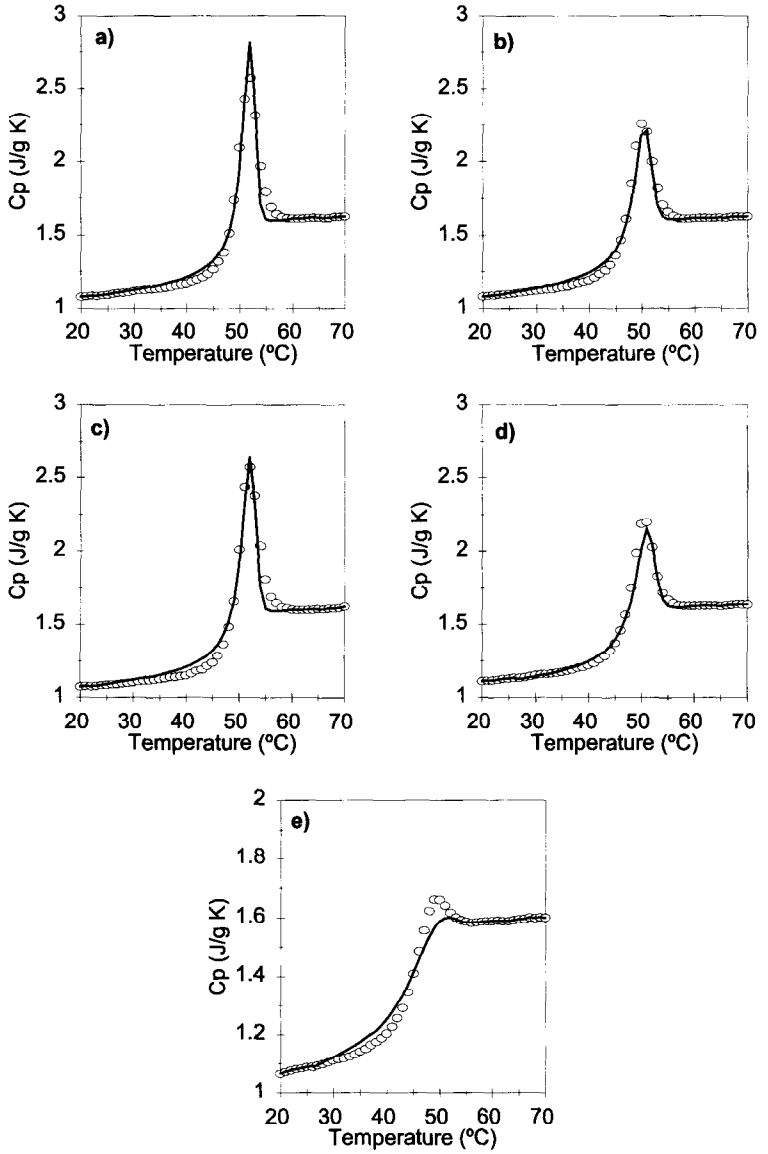

Fig. 2. Experimental thermograms measured for PVAc after thermal histories that include an isothermal annealing at 25°C for 332 min (Fig. 2*a*), 30°C for 90 min (Fig. 2*b*) and 370 min (Fig. 2*c*), and 35°C for 735 min (Fig. 2*d*). The result of the scans measured after cooling at 40 K min^{-1} (Fig. 2*e*) is also included. The solid line represents the prediction of the model with $B = 1000\ J\ g^{-1}$ and the remaining parameters according to Table 1

in terms of the temperature dependence of the heat capacity, $c_p(T)$, calculated from the heat flux output of the DSC. The heat capacity standard was sapphire. For the reference scan, t_a was zero.

3. Results and discussion

3.1. Experimental results and model simulation

Fig. 2 shows five $c_p(T)$ curves measured after different thermal histories. These curves are some of the ones employed in reference [21] to calculate the time and temperature dependence of the enthalpy change during the isothermal annealing: $\Delta h(T_a,t_a)$.

We will take as the glass transition temperature of our PVAc sample, $T_g = 42°C$, which is the temperature of the crossing point of the enthalpy lines corresponding to the liquid and glassy states calculated by integration of the reference scan. The experimental data of the heat capacity at temperatures well above and below the glass transition were fitted to straight lines to determine the temperature dependence of c_{pl} and c_{pg} respectively. The temperature dependence of the configurational heat capacity was calculated as an average of the lines determined in all the thermograms, giving $\Delta c_p = 0.8525 - 0.001381\ T\ J\ g^{-1}\ K^{-1}$ with T in K.

The parameters of the model are supposed to be material parameters, independent of the thermal history. The model with a single set of parameters should be able to reproduce the $c_p(T)$ curves measured after any thermal history. Thus, the set of parameters was determined by simultaneous least squares fit to the $c_p(T)$ curves shown in Fig. 2, whose

Table 1
Model parameters found with $S_c^{lim}(T)$ as in Fig. 1 for each value of B

B(J g^{-1} K^{-1})	δ	β	ln$A(s)$	T_2(°C)	$T_g - t_2$(°C)
500	0.17	0.41	− 22.5	2.1	39.9
1000	0.17	0.45	− 31.3	− 14.3	56.3
1500	0.17	0.47	− 36.7	− 27.9	69.9
2000	0.17	0.50	− 41.0	− 38.9	80.9
2500	0.17	0.52	− 44.6	− 48.5	90.5
3000	0.17	0.54	− 47.5	− 57	99.0

thermal histories are considered to cover a broad enough range of annealing temperatures and times. Due to the correlation existing between B, T_2 and ln$A$, the value of B was first fixed and a least-squares routine was used to determine the set of four parameters, δ, β, T_2 and ln$A$, that yield a model simulated set of $c_p(T)$ curves as close as possible to the set of five experimental $c_p(T)$ curves shown in Fig. 2. This procedure was repeated with different values of B, ranging between 500 and 3000 J g^{-1}. In this way, different sets of model parameters are found (Table 1). In Fig. 2, the full lines show the model calculations with $B = 1000$ J g^{-1}, with the rest of parameters according to Table 1. The model simulation of any of the thermal histories corresponding to Fig. 2a–d leads to almost indistinguishable $c_p(T)$ curves when conducted with the different sets of parameters shown in Table 1, i.e. for the different values of B. This is due to the correlation that exists between B, T_2 and ln$A$, in such a way that the different sets of parameters lead to very similar values of the relaxation times in the temperature interval that is significant in the experiments. As an example, Fig. 3 shows the temperature dependence of the relaxation times in equilibrium, calculated with values of B of 1000 and 3000 J g^{-1}. These curves are quite similar in the temperature interval that is relevant in the experiments.

There is a significant difference in the model prediction of the reference scan using the different values of B (Fig. 4). Low values of B do not predict the small overshoot appearing in this $c_p(T)$ curve, however, the curve calculated with high values of B shows good agreement with the experimental data. It is important to note that this does not mean that the model has a particular difficulty in reproducing the $c_p(T)$ curves measured after this particular thermal history: the simultaneous least squares fit gives the set of parameters for which the overall approach of the five calculated curves to the experimental ones is the best.

The value of δ is independent of B as shown in Table 1. This parameter determines the value of the entropy in the limit states of the structural relaxation process. The most important difference between the model for the structural relaxation we have used in this work and the SH or NM models is the difference assumed between the configurational entropy in the limit states and that of the equilibrium states at the same temperature. The model also predicts that the enthalpy in the limit states of the structural relaxation are higher than those of the equilibrium states. This feature could, in principle, be experimentally checked, as the increment of enthalpy during the isothermal annealing $\Delta h(T_a,t_a)$ can be calculated from the kind of curves shown in Fig. 2 (see for instance references [22] and [23]). The problem comes from the experimental time needed to attain a steady state (a value of $\Delta h(T_a,t_a)$ independent of the annealing time) in the isothermal structural relaxation process.

The experimental $\Delta h(T_a,t_a)$ data in the literature, on which to base the conclusion that a material has reached its limit state during the isothermal annealing process, are scant. For a maximum ageing time of 10^4 min it seems that such results are to be found only in a narrow temperature interval between T_g (determined as the intercept temperature of the liquid and glass enthalpy lines) and $T_g - (7 \div 10)°$. The experimental data reported by Cowie et al. [21] for

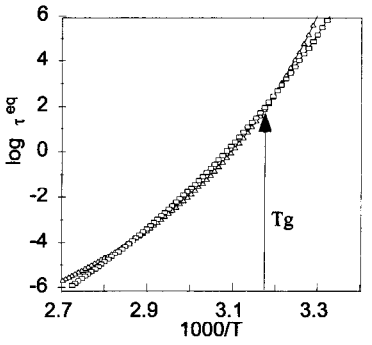

Fig. 3. Temperature dependence of the relaxation times in equilibrium determined by the model for different values of B (see text); (Δ) 1000 J g^{-1} and (□) 3000 J g^{-1}

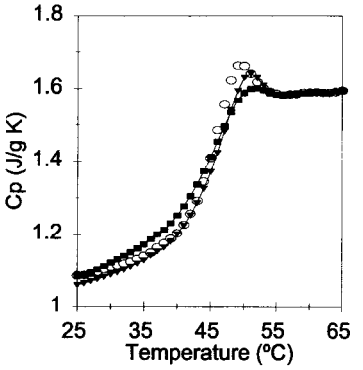

Fig. 4. Thermograms predicted by the model for the reference scan. The experimental data are represented as open circles. The model calculations with $B = 1000$ (■) and 3000 J g^{-1} (▼) (and the rest of the parameters as in Table 1 for each value of B) are represented

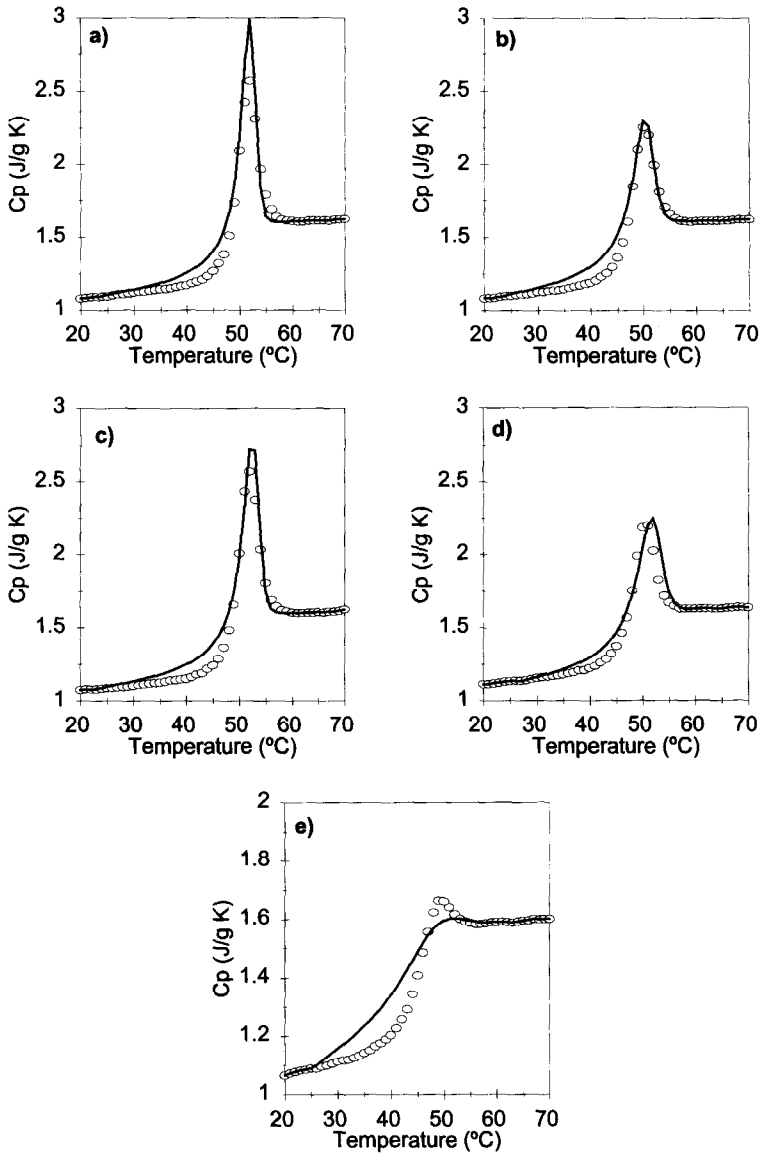

Fig. 5. Experimental thermograms measured for PVAc after thermal histories that include an isothermal annealing at 25°C for 332 min (Figure 2*a*), 30°C for 90 min (Figure 2*b*) and 370 min (Figure 2*c*), and 35°C for 735 min (Figure 2*d*). The result of the scans measured after cooling at 40 K min^{-1} (Figure 2*e*) is also included. The solid line represents the model simulation with the assumption $S_c^{lim}(T) = S_c^{eq}(T)$ and the set of parameters: $B = 1000$ J g^{-1}, $\beta = 0.40$, $T_2 = -22$°C, $\ln(A/s) = -27.0$

PVAc allow us to determine values of $\Delta h(T_a,\infty)$ at $T_g - 7$ and $T_g - 10$, that are smaller than the respective equilibrium values predicted for equilibrium:

$$\Delta h^{eq}(T_a) = \int_{T_a}^{T_g} \Delta c_p(T)\mathrm{d}T$$

(see Table 2). The data of $\Delta h(T_a,\infty)$ reported by Algería et al. [24] in a similar interval of annealing temperatures, agree very well with the values of reference [21]. At lower ageing temperatures, the limit state cannot be attained within the experimental time interval. It has been suggested that the limit values for lower ageing temperatures should be estimated on the basis of shorter time enthalpy loss data and a model equation [23,25,26]. Extrapolated values of $\Delta h(T_a,\infty)$ at $T_g - 12$ and $T_g - 17$ were obtained with this procedure showing values again smaller than the equilibrium ones.

The limit values predicted by the model for $\Delta h(T_a,t_a)$ can be calculated from the equation:

$$\Delta h^{lim}(T_a) = \int_{T_a}^{T_g} \Delta c_p^{lim}(T)\mathrm{d}T.$$

The value of the parameter δ, determined in the search routine, leads to the values for $\Delta h^{lim}(T_a)$ shown in Table 2, in good agreement with the estimations of reference [21].

If the value of δ is kept fixed and equal to zero in the least squares routine, i.e., if one assumes that $S_c^{lim}(T) = S_c^{eq}(T)$, the fit is significantly poorer, as shown in Fig. 5. It is noteworthy that, in this case, the equations of the model became

Table 2
Enthalpy data at the limit of the isothermal structural relaxation process

Ageing temperature	$\Delta h(T_a,\infty)$(J g^{-1})[a]	$\Delta h^{lim}(T_a)$(J g^{-1})	$\Delta h^{eq}(T_a)$(J g^{-1})
$T_g - 7$	1.8	1.8	3.0
$T_g - 10$	2.5	2.7	4.3
$T_g - 12$	3.0	3.2	5.1
$T_g - 17$	4.2	4.6	7.3

[a] Experimental or extrapolated data taken from Ref. [21] (see text).

very similar to those of the SH model. The differences then lie in the form of the temperature dependence of the configurational heat capacity and in the fact that, in the model used in this work, the experimental thermograms are not converted to dT_f/dT curves. However, these facts seem not to be critical in the quality of the model fit [15]. Thus, the improvement in the fit with respect to the SH model has to be ascribed to the difference between the configurational entropy in the limit states and in the equilibrium states.

3.2. The size of the cooperative rearranging region from the Adam–Gibbs theory

The application of the Adam–Gibbs theory to amorphous polymers needs an interpretation of the CRR in terms of main-chain polymer segments. We define a chain segment as a number of consecutive main-chain bonds, large enough to allow a conformational transition in the isolated segment when the position of the two atoms in its both ends are fixed. The number of main-chain bonds in a segment can be close to that of the crankshaft mechanism, but, as we will show below, it is not very important for the arguments given in this work. It is possible to define a chain segment for each main-chain bond, allowing several segments to overlap each other, an idea similar to that of the model proposed by Robertson [1]. With reference to the scheme of Fig. 6, if the number of bonds per segment is six, the sequence C1-C2-C3-C4-C5-C6-C7 would constitute a chain segment and C2-C3-C4-C5-C6-C7-C8 would be a different one. The CRR consists of a number, z, of close packed segments.

To estimate the value of $\Delta\mu'$, a PVAc chain segment was modelled using a methyl-terminated, tetramer sequence. There are six distinguishable tetramers; *mmm*, *mmr*, *rmr*, *mrm*, *rrm* and *rrr*, where *r* is a racemic and *m* is a meso dyad; Fig. 6 shows an example, using the *rrm* tetramer, with the atoms numbered.

The two central bonds C4-C5 and C5-C6 are taken as representative of the energy states of the six possible configurational situations. The energy profiles were obtained by rotating the dihedral angles C3-C4-C5-C6 and C4-C5-C6-C7 using Allinger's [27] molecular modelling program MMP2, starting from a minimum energy position. The energy profiles were calculated for different segment lengths. Fig. 7 shows the energy profiles obtained by rotating the dihedral angle C4-C5-C6-C7 in the *mmm* tetramer fixing C1, C2, C3, C7, C8 and C9 (four main chain bonds per segment), fixing the atoms C1, C2, C8 and C9 (six main chain bonds per segment), and fixing the position of C1 and C9 (eight main chain bonds per segment). The calculations performed, which allow the free motion of both ends of the model tetramer, are also shown. The energy barriers decrease as the number of free bonds increases, rapidly approaching those calculated when allowing for free motion of both extremes of the tetramer (Table 3 shows the average energy barriers of the two bond rotations). We will use here the last calculations as representative of the main chain segments involved in the cooperative rearrangements. the results of these molecular modelling calculations are summarized in Table 4.

The minimum energy is obtained with this particular tetramer in an all-trans configuration ($\pm$ ~175°). Separately flexing each of the centre bonds into their gauche configurations gives the expected two higher energy states; g − is located at around − 70° and g + at around 75°.

The possible configurational transitions in each tetramer cannot be characterized by a single rotational barrier as it is assumed in the Adam–Gibbs theory. Eq. (1) is interpreted in the sense that a conformational rearrangement inside a CRR involves z^* simultaneous or sequential jumps with energy barrier, $\Delta\mu$. Due to the appearance of the product $z^*\Delta\mu$ in Eq. (1), it makes sense to take the average of the barriers hindering all the possible transitions in our model tetramer for $\Delta\mu$. This implies that the probability of each individual jump depends more on the spacial arrangement of the neighbor polymer chains in the CRR than on the specific value of

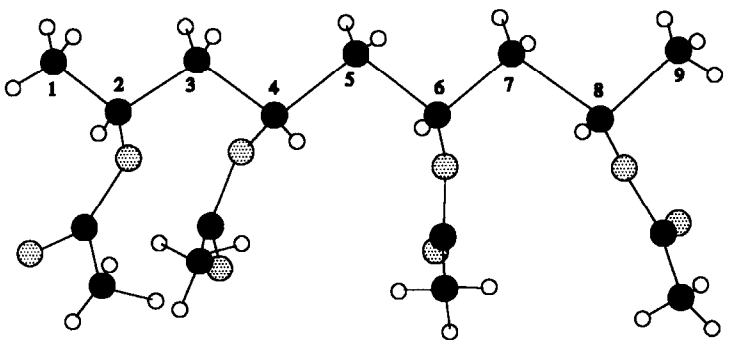

Fig. 6. Scheme of the vinyl acetate tetramer used in molecular mechanics calculations

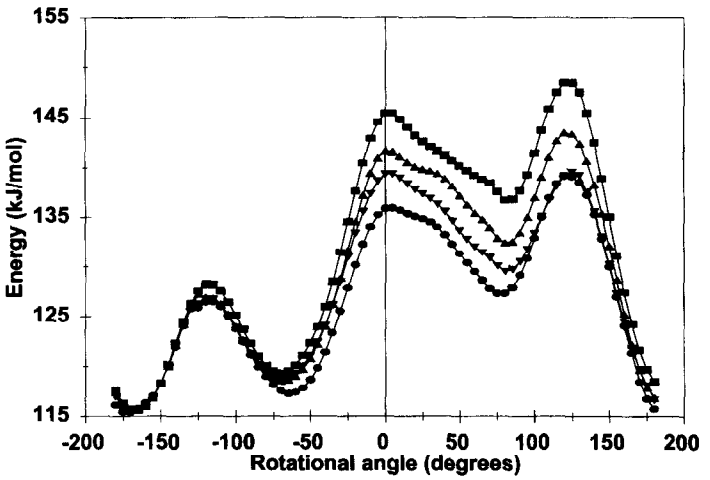

Fig. 7. Rotational potential energy for the *mmm* vivyl acetate tetramer. Calculations performed fixing C1, C2, C3, C7, C8 and C9 (squares), fixing the atoms C1, C2, C8 and C9 (triangles), and fixing the coordinates position of C1 and C9 (inverted triangles). The calculations performed which allowed the free motion of both ends of the model tetramer are also shown (circles)

the energy barrier. In this work, an average value $\Delta\mu' = 14.6$ kJ mol^{-1} has been used. The different probability of each tetramer sequence was considered in the calculation of the average value of $\Delta\mu'$ as explained in [21].

All the calculations have been performed considering only intramolecular interactions. Obviously the intermolecular interactions play an important role in the conformational rearrangements. Around a given chain segment there are molecular groups pertaining to the neighbour chain segments. It can be considered that these molecular groups are randomly distributed in space in such a way that they could affect the absolute values of the potential energy in any state but not the rotational barriers hindering the conformational motions.

The effect of the close packing of the polymer chain segments in the CRR is to diminish greatly the number of available rotational states of the chain segments. Many of the possible conformations of a chain segment are, in fact, not available, since the positions that the segment atoms should occupy after the transition are already occupied by atoms of different chain segments, that are themselves inmobile. Thus, a CRR containing z^* segments with three possible rotational states for each one, could have 3^{z^*} states, if no intermolecular interactions exist. This big number is reduced to a small number Ω^*, due to the close packing of the main chain segments inside the CRR.

From Eqs. (2) and (4), it is possible to find a direct relationship between parameter B and Ω^*:

$$\ln\Omega^* = \frac{BM_s}{\Delta\mu'} \tag{14}$$

Adam and Gibbs [4] mentioned that Ω^* could take the value of two, with just one state available for the CRR before the conformational transition and another one after it. Hodge [12] proposed a higher value $3! = 6$. Since one chain segment can be defined for each main chain bond, a molecular weight of $M_s = 43$ g mol^{-1} (a half of the molecular weight of the monomeric unit) has been used for the chain segment.

Eq. (2) can be applied at the glass transition temperature to give the value of $z^*(T_g)$, and the configurational entropy at T_g was calculated using Eq. (13), with the values of T_2 obtained with the curve fitting routine. Table 5 gives the values of Ω^* and $z^*(T_g)$ as a function of B.

The value of Ω^* can be taken as the basis to establish a criterium to decide the value of the parameter, B, independently from the curve fitting calculation. It appears clearly that Ω^* rapidly increases with B. High values of Ω^* are not reasonable for the smallest CRR and from this point of view, values of B equal to or higher than 1500 J g^{-1} can be ruled out in this polymer. It is very significant that the set of parameters found by the search routine with $B = 1000$ J g^{-1}, determine relaxation times that agree very well with the features generally accepted for the main viscoelastic or dielectric relaxation processes.

The dielectric and viscoelastic relaxation times are usually expressed in terms of Eq. (5). In reference [28], data for the difference $T_g - T_0$, taken from different authors, are collected, showing values between 57 and 58.4°, which

Table 3
Energy barriers for the transitions between trans (t), gauche + (g^+) and gauche − (g^-) conformations of the *mmm* VAc tetramer calculated fixing the position of different atoms of the main chain. The atoms are numbered according to the schema of figure 6 (see text). The average of the bond rotations C4–C5 and C5–C6 is considered

Main-chain atoms fixed in the calculations	$t \rightarrow g^-$	$g^- \rightarrow t$	$g^- \rightarrow g^+g^+ \rightarrow g^-g^+ \rightarrow t$		$t \rightarrow g^+$	
C1, C2, C3, C7, C8, C9	14.7	10.2	28.8	19.9	8.8	22.3
C1, C2, C8, C9	14.1	10.0	26.1	19.3	8.0	18.9
C1, C9	13.2	11.1	22.7	16.4	8.7	17.1
Free ends	13.0	11.6	21.5	15.6	8.6	15.9

Table 4
Energy barriers for the transitions between trans (t), gauche + (g^+) and gauche − (g^-) conformations of the different VAc tetramers (see text). The average of the bond rotations C4–C5 and C5–C6 is considered

Tetramer	P_{iii}	$t \rightarrow g^-$	$g^- \rightarrow t$	$g^- \rightarrow g^+$	$g^+ \rightarrow g^-$	$g^+ \rightarrow t$	$t \rightarrow g^+$
mmm	0.125	13.0	11.6	21.5	15.6	8.6	15.9
mmr	0.25	12.8	12.5	21.5	14.2	8.1	15.6
rmr	0.125	14.8	9.1	16.6	14.8	8.9	16.3
mrm	0.125	25.7	16.1	15.0	14.9	4.7	14.4
rrm	0.25	13.2	5.1	18.8	18.6	16.3	24.5
rrr	0.125	7.5	4.3	22.6	14.7	10.7	22.0

agrees with the value of $T_g - T_2 = 56.3$ found in our curve fitting routine with $B = 1000\ J\ g^{-1}$. The identification of T_2 and T_0 can be justified by the representation of the calorimetric relaxation times calculated from Eq. (12) in the $\ln\tau^{eq}$ versus $1/(T - T_2)$ plot (see Fig. 8), with the straight line found also allowing us to determine $DT_0 = 2031$ K and $D = 7.9$. This value of D corresponds to a fragile, glass-forming system in the framework of Angell's [3] classification, as it should. The preexponential factor found with $B = 1000\ J\ g^{-1}$, $A = 2.6\ 10^{-14}$ s, is also the value that can be expected for the limit of the relaxation times at infinite temperature.

The β parameter of the KWW equation agrees with the values obtained from viscoelastic experiments, around 0.42–0.43 (see reference [28] and the references there cited). In dielectric experiments, the parameter β is found to significantly increase with decreasing temperature [29,30], with values ranging between 0.51 and 0.64. Ngai et al. [28] found that the product βC is the same when determined from different experimental techniques, with a value around 900 K. From our DSC experiments, with $B = 1000\ J\ g^{-1}$, we find $\beta C = 914$ K.

Lower values of the parameter B lead to smaller Ω^*, close to the values proposed by Hodge, or Adam and Gibbs. However, the values found by the search routine for the difference $T_g - T_2$ and the preexponential factor A for $B = 500\ J\ g^{-1}$ seem less realistic than those found with $B = 1000\ J\ g^{-1}$. This indicates that the CRR could have a number of possible states slightly higher than those proposed by Hodge, and Adam and Gibbs.

The size z^* of the CCR, accepting $B = 1000\ J\ g^{-1}$, is

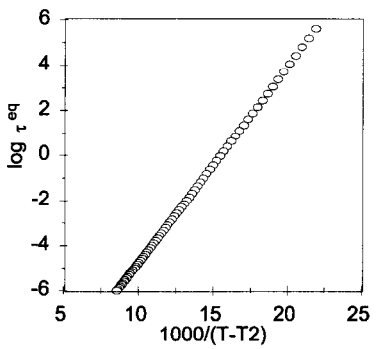

Fig. 8. Equilibrium relaxation time calculated with $B = 1000\ J\ g^{-1}$.

Table 5
Parameters related to the size of the smallest CRR at T_g as obtained from the Adam–Gibbs theory

B(J g^{-1} K^{-1})	$S_c(T_g)$(J g^{-1} K^{-1})	z^*	Ω^*
500	0.060	4.8	5
1000	0.090	6.4	20
1500	0.117	7.4	88
2000	0.141	8.2	392
2500	0.164	8.8	1746
3000	0.185	9.4	7772

equal to 6.4. This means that a cooperative rearrangement involves the simultaneous or sequential movement of six main chain segments. The number of repeating units of the main chains involved in such cooperative motion remains uncertain, as the definition of the main chain segments allows them to overlap each other, but it can be said that this number is around 20. If all the segments pertain to different polymer chains and each segment contains eight bonds, the CRR would contain around 25 repeating units of the main chain. However, if some of the segments pertain to the same polymer chain, then this number is reduced.

3.3. The size of the cooperative rearranging region from the temperature fluctuation theory

Another approach to the size of the CRR is the formula proposed by Donth [2,31] to relate the volume of the CRR with the mean temperature fluctuation in this region at T_g:,

$$V_a = kT_g^2\Delta(1/c_v)/\rho\delta T^2. \quad (15)$$

where V_a is the volume of the CRR, $\Delta(1/c_v) = 1/c_{vg} - 1/c_{vl}$, with c_{vg} and c_{vl} being the specific heat at constant volume of the glass and the liquid, respectively, at T_g, ρ is the density and δT is the mean temperature fluctuation in the CRR.

The temperature fluctuation can be determined from the mean fluctuation in $\ln\tau$, δq, that, in turn, can be evaluated from the β parameter of the KWW equation through:

$$\delta q = \frac{1.04 \pm 0.05}{\beta}.$$

The relationship between δT and δq comes from:

$$\frac{\delta q}{\delta T} = -\frac{1}{T_g^2}\left(\frac{d\ln\tau^{eq}}{d(1/T)}(T_g)\right)$$

The values of the specific heat at constant volume at T_g were calculated from the corresponding values of the specific heats at constant pressure from the well known formula:

$$c_v = c_p - \frac{T\alpha^2}{\rho\gamma}.$$

The values of the expansion (α) and compressibility (γ) coefficients and the density (ρ) at T_g were taken from the data of McKinney and Goldstein [32], as explained in [21],

leading to $c_{vg}(T_g) = 1.063\ J\ g^{-1}\ K^{-1}$, $c_{vl}(T_g) = 1.290\ J\ g^{-1}\ K^{-1}$ and $\rho(T_g) = 1.186\ g\ cm^3$./

Thus, from the model parameters found with $B = 1000\ J\ g^{-1}$ we find $\delta T = 3.65\ K$ and $V_a = 14.3\ nm$. This CRR would contain 119 monomeric units, which is higher, but still within an order of magnitude, of what we deduced from the Adam–Gibbs theory above. The correlation length can be calculated from the volume of the CRR:

$$\xi_a = V_a^{1/3} = 2.4 nm,$$

which agrees with the value determined by Donth [2] for this polymer from the results of Sasabe and Moynihan [29] and by Donth et al. [33] using different approaches.

Acknowledgements

The work of the group of the Universidad Politécnica de Valencia was partially supported by CICYT through the project MAT94-0596. J. L. G. R. wishes to thank the Spanish DGICYT and the Royal Society of London for supporting his stay at the Heriot–Watt University during the summer of 1996.

References

[1] Robertson RE. J Polym Sci Polym Phys Ed 1979;17:597.
[2] Donth E. J Non-Cryst Solids 1982;53:325.
[3] Angell CA. J Non-Cryst Solids 1991;3:131–133.
[4] Adam G, Gibbs JH. J Chem Phys 1965;43:139.
[5] Miller AA. J Chem Phys 1968;49:1393.
[6] Davies RO, Jones GO. Adv Phys 1953;2:370.
[7] Hodge IM. J Non-Cryst Solids 1994;169:211.
[8] Scherer W. J Non-Cryst Solids 1990;123:75.
[9] McKenna GB. J Res Natl Inst Stand Technol. 1994;99:169.
[10] Hutchinson JM. Prog Polym Sci 1995;20:703.
[11] Scherer GW. J Am Ceram Soc 1984;67:504.
[12] Hodge IM. Macromolecules 1987;20:2897.
[13] Narayanaswamy OS. J Am Ceram Soc 1971;54:491.
[14] Moynihan CT, Macedo PB, Montrose CJ, Gupta PK, DeBolt MA, Dill JF, Dom BE, Drake PW, Easteal AJ, Elterman PB, Moeller RP, Sasabe H. Ann NY Acad Sci 1976;279:15.
[15] Gómez Ribelles JL, Monleón Pradas M. Macromolecules 1995;28:5867.
[16] Gómez Ribelles JL, Monleón Pradas M, Más Estellés J, Vidaurre Garayo A, Romero Colomer F, Meseguer Dueñas JM. Polymer 1997;38:963.
[17] Brunacci A, Cowie JMG, Ferguson R, Gómez Ribelles JL, Vidaurre A. Macromolecules 1996;29:7676.
[18] Montserrat S, Gómez Ribelles JL, Meseguer Dueñas JM. Polymer 1998;39:3801.
[19] Meseguer Dueñas JM, Vidaurre Garayo A, Romero Colomer F, Más Estellés J, Gómez Ribelles JL, Monleón Pradas M. J Polym Sci Polym Phys Ed 1997;35:3201.
[20] Gibbs JH, DiMarzio EA. J Chem Phys 1958;28:373.
[21] Cowie JMG, Harris S, McEwen IJ. Polymer 1997;35:1107.
[22] Gómez Ribelles JL, Ribes Greus A, Díaz Calleja R. Polymer 1990;31:223.
[23] Cowie JMG, Ferguson R. Polymer 1993;34:2135.
[24] Algería A, Guerrica-Echevarría E, Goitiandía L, Tellería I, Colmenero J. Macromolecules 1995;28:1516.
[25] Cowie JMG, Ferguson R. Polymer Commun 1986;27:258.
[26] Cowie JMG, Ferguson R. Macromolecules 1989;22:2307.
[27] Allinger NL. MMP2(85), QCPE, University of Indiana, Bloomingfield, IN, 1985.
[28] Ngai KL, Mashimo S, Fytas G. Macromolecules 1988;21:3030.
[29] Sasabe H, Mohynihan CT. J Polym Sci Polym Phys Ed 1978;16:1447.
[30] Nozaki R, Mashimo S. J Chem Phys 1986;84:3575.
[31] Donth E. Relaxation and thermodynamics in polymers, glass transition. Berlin: Akademie, 1992.
[32] McKinney JE, Goldstein M. J Res Natl Bur Stand 1974;17A:331.
[33] Donth E, Beiner M, Reissing S, Korus J, Garwe F, Vieweg S, Kahle S, Hempel E, Schröter K. Macromolecules 1996;29:6589.